UNIVERSITY *of* York

This is a repository copy of *Decay modes of the 9/2- isomeric state in 183Tl*.

Article:

Venhart, M., Andreyev, A. N. orcid.org/0000-0003-2828-0262, Cubiss, J. G. orcid.org/0000-0002-5076-8654 et al. (24 more authors) (2022) Decay modes of the 9/2- isomeric state in 183Tl. Phys. Rev. C. 034338. ISSN 2469-9993

Decay modes of the 9/2− isomeric state in ¹⁸³Tl

M. Venhart [1,*] A. N. Andreyev,[2,3] J. G. Cubiss,[2] J. L. Wood,[4] A. E. Barzakh,[5] C. Van Beveren,[6] T. E. Cocolios,[6] R. P. de Groote,[6] D. V. Fedorov,[5] V. N. Fedosseev,[7] R. Ferrer,[6] D. A. Fink,[7,8] L. Ghys,[6,9] M. Huyse,[6] U. Köster,[10] J. Lane,[11] V. Liberati,[11] K. M. Lynch,[7,12] B. A. Marsh,[7] P. L. Molkanov,[5] T. J. Procter,[12] E. Rapisarda,[6] K. Sandhu,[11] M. D. Seliverstov,[2,5,7,11] A. M. Sjödin,[7] P. Van Duppen,[6] and M. Veselský[13]

¹*Institute of Physics, Slovak Academy of Sciences, SK-84511 Bratislava, Slovakia*
²*Department of Physics, University of York, York YO10 5DD, United Kingdom*
³*Advanced Science Research Center (ASRC), Japan Atomic Energy Agency (JAEA), Tokai-mura, Ibaraki 319-1195, Japan*
⁴*Department of Physics, Georgia Institute of Technology, Atlanta, Georgia 30332, USA*
⁵*Petersburg Nuclear Physics Institute, NRC Kurchatov Institute, 188300 Gatchina, Russia*
⁶*KU Leuven, Instituut voor Kern- en Stralingsfysica, B-3001 Leuven, Belgium*
⁷*CERN, CH-1211, Geneva 23, Switzerland*
⁸*Ruprecht-Karls Universität, D-69117 Heidelberg, Germany*
⁹*Belgian Nuclear Research Centre SCK CEN, Boeretang 200, B-2400 Mol, Belgium*
¹⁰*Institut Laue Langevin, 6 rue Jules Horowitz, F-38042 Grenoble Cedex 9, France*
¹¹*School of Engineering and Science, University of the West of Scotland, Paisley PA1 2BE, United Kingdom*
¹²*The University of Manchester, School of Physics and Astronomy, Oxford Road, Manchester M13 9PL, United Kingdom*
¹³*Institute of Experimental and Applied Physics, Czech Technical University, CZ-110 00 Prague, Czech Republic*

The internal transition decay and α decay of the $T_{1/2} = 53.3$ ms, $9/2^-$ isomeric state in the neutron-deficient isotope, ¹⁸³Tl, have been studied using the Resonance Ionization Laser Ion Source and the Windmill detection setup at the ISOLDE facility at CERN. Clean samples of ¹⁸³ᵐTl were produced by selective laser ionization and subsequent mass separation. An internal transition cascade of 356.5–272.2 keV γ rays has been identified. Multipolarities of these transitions have been determined by means of simultaneous γ-ray and conversion-electron spectroscopy. Improved data for the fine structure of the ¹⁸³ᵐTl $\rightarrow$ ¹⁷⁹Au decay were deduced. This involves a 6058 keV α-decay transition, which populates a previously unknown state in ¹⁷⁹Au, that is tentatively assigned as a $(9/2^-)$. It is interpreted as a coupling of the $1h_{9/2}$ proton-intruder with the excited 0^+ state in the ¹⁷⁸Pt core.

I. INTRODUCTION

The very neutron-deficient region around $Z = 82$ is the best and most extensively characterized example of low-energy shape coexistence in nuclei [1–3]. While detailed information on the heavy isotopes in the lead region is available, the current focus is on the lighter isotopes: this is critical in order to establish detailed knowledge on nuclear structure with respect to the shape coexisting states. These light isotopes are a challenge for experimental studies. In order to get a more microscopic understanding of shape coexistence, detailed spectroscopy information is necessary. However, because of the weak radioactive beam intensities and the fact

*Corresponding author: martin.venhart@savba.sk

that they are in most cases overwhelmed by unwanted more stable isotopes, these studies are hampered. With recent developments of laser ionization sources [4], clean beams of very neutron-deficient isotopes are available and thus such studies are now possible.

Neutron-deficient Tl isotopes display an extensive example of nearly degenerate shape coexistence [1,2,5]. The odd-mass Tl isotopes have $1/2^+$ near-spherical ground states and deformed $9/2^-$ so-called intruder states [6,7]. The first-excited state in these Tl isotopes had spin-parity $3/2^+$, except for ¹⁸⁹Tl. The systematics of these states are shown in Fig. 1. Positive-parity states are associated with the $3s_{1/2}$ and $2d_{3/2}$ proton-hole configurations, where the odd protons couple to the even-mass Pb cores. The decay of the $3/2^+$ state to the $1/2^+$ ground state proceeds through a mixed $M1 + E2$ transitions with dominant $E2$ components.

Next to these states associated with the proton-hole configurations, proton particle $1h_{9/2}$, $2f_{7/2}$, and $1i_{13/2}$ configurations (above the $Z = 82$ shell closure) occur in the low-excitation spectrum of odd-mass Tl isotopes [8–11]. These states, associated with proton excitation across the $Z = 82$ proton
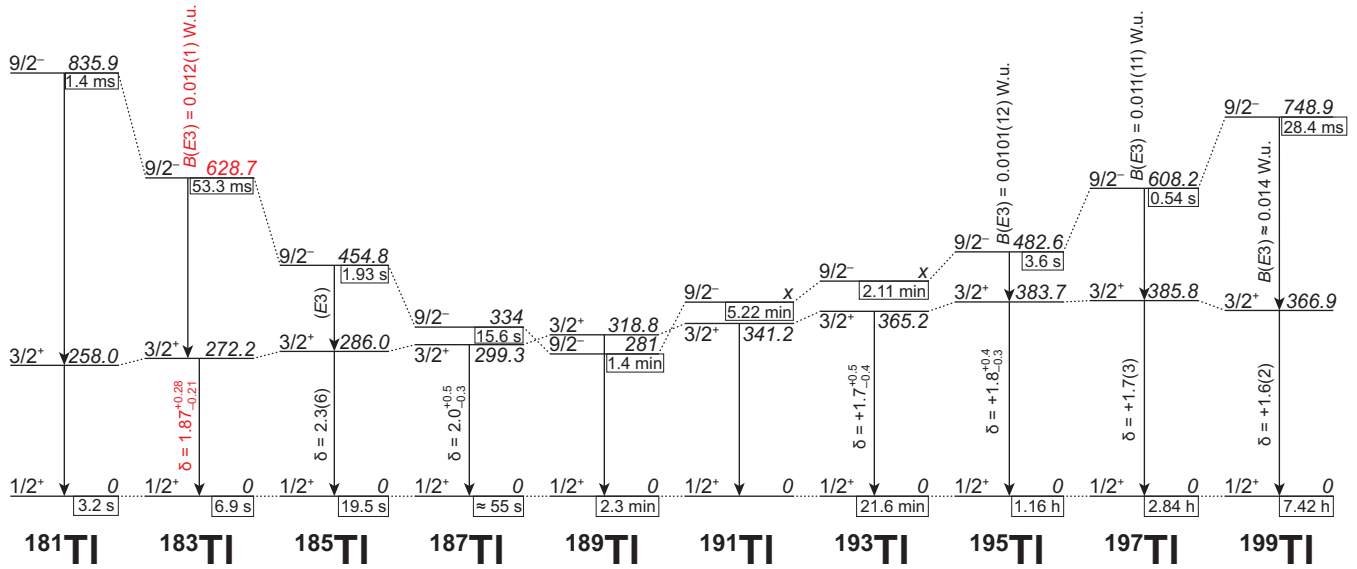
FIG. 1. Systematics of $1/2^+$, $3/2^+$, and $9/2^-$ states in neutron-deficient odd-mass Tl isotopes. The $3/2^+ \rightarrow 1/2^+$ transitions have $M1 + E2$ mixed character and their mixing ratios δ are given. The $9/2^- \rightarrow 3/2^+$ transitions have $E3$ multipolarity. Data determined in the present work are highlighted with red color, other data are taken from Evaluated Nuclear Structure Data File.

shell closure 'intrude' in the low-energy excitation spectrum because of massive correlations resulting from the changing shell occupancies. This leads to a characteristic "parabolic" pattern of the excitation energy as a function of neutron number [1]. Most notably, $9/2^-$ states associated the $1h_{9/2}$ configuration, described as coupled to 0^+ ground states of respective even-mass Hg cores, form an uninterrupted isomeric chain between ^{201}Tl and ^{181}Tl, see Fig. 1. Strongly coupled rotational bands based on these isomers were observed [8–11], indicating their oblate deformation with dominant $9/2^-$[505] Nilsson configuration.

Predominantly, these $9/2^-$ isomers in odd-mass Tl isotopes de-excite via $E3$ transitions that feed the $3/2^+$ states [5,12–17]. The reduced transition probabilities of these $E3$ transitions are of the order of 0.01 W.u. Weak α-decay branches were reported for the $9/2^-$ isomers in ^{181,183,185,187}Tl [5,9,18–20].

Decoupled prolate bands, based on a second $9/2^-$ state, were observed in ^{183,185,187}Tl [8,9]. These second $9/2^-$ states occur due to the coupling of the $1h_{9/2}$ proton with coexisting excited 0^+ states [21] in ^{182,184,186}Hg cores. The mixing of two differently deformed $9/2^-$ states is expected. This has been suggested for the first time in the shape coexistence review, see Fig. 18 in [1]. The increase of the isomer shift for the $9/2^-$ state in ^{183}Tl, reported by the in-source laser spectroscopy experiment [7], suggests its larger deformation and thus corroborates the proposed prolate-oblate mixing for the $9/2^-$ isomer in ^{183}Tl.

The present article reports on results of an experiment carried out to study an internal transition and the α decay of the short-lived ($T_{1/2} = 53.3(4)$ ms [9]) $9/2^-$ isomeric state in ^{183}Tl, denoted as ^{183m}Tl in further text. The ground state of ^{183}Tl has a much longer half-life of 6.9(7) s [22]. The experiment has been conducted as a part of a focused campaign at the Isotope Separator On-Line Device (ISOLDE) at

CERN studying the decay properties and intrinsic structure of neutron-deficient Tl isotopes [7,21,23–26].

The ^{183}Tl α decay has been identified using the online mass separator at GSI Darmstadt [18]. Three α-decay energies of 6343(10), 6378(15) and 6449(15) keV were reported, but no decay scheme was given.

Another study, performed at the RITU gas-filled separator at the University of Jyväskylä, proposed a decay scheme for the ^{183m}Tl $\rightarrow$ ^{179}Au α decay. It includes 52.4, 61.8, and 89.4 keV coincident γ rays. This level scheme has been adopted for the most recent Evaluated Nuclear Structure Data File (ENSDF) for ^{179}Au, see [27].

A significantly different level scheme has been constructed on a basis of combined data acquired at RITU separator and at ISOLDE [19]. This involved a discovery of the 328 ns isomeric state in ^{179}Au. It was shown that the 6378(15) keV transition reported in [9,18] was an artefact due to the α-electron summing effect. Note that the level scheme given in [19] presently does not appear in the ENSDF, however it is reported in the experimental unevaluated nuclear data list (XUNDL).

In the present work, a more substantial decay scheme, which extends the one proposed in [19], was constructed for the ^{183m}Tl $\rightarrow$ ^{179}Au α decay.

In a study of the ^{187}Bi $\rightarrow$ ^{183}Tl α decay at velocity filter SHIP at GSI Darmstadt, a $3/2^+$ first-excited state with an excitation energy of 273(1) keV was identified in ^{183}Tl, together with a corresponding $3/2^+ \rightarrow 1/2^+ \gamma$-ray transition [28].

In the same study at SHIP, an excitation energy of 625(7) keV and an α-decay branching ratio of 1.5(3)% was determined for ^{183m}Tl. The missing decay strength was interpreted as an internal transition decay [22], however, corresponding γ rays were not observed. A cascade of γ rays depopulating ^{183m}Tl was identified for the first time in the present work. Multipolarities of both transitions

were unambiguously determined by means of γ-ray and conversion-electron spectroscopy.

II. EXPERIMENTAL DETAILS

The experiment was performed at the ISOLDE facility at CERN. A proton beam with an energy of 1.4 GeV and intensity up to 2.1 μA impinged upon thick 50 g/cm^2 UC$_x$ target, producing ^{183}Tl nuclei via the spallation process. The proton beam was delivered by the Proton Synchrotron Booster (PSB) accelerator in a repeated sequence of 34 pulses, separated by 1.2 s periods. This sequence is referred to as a supercycle. After proton impact, recoiling nuclei stopped in the target material, subsequently diffused out of the high-temperature target material as neutral atoms and effused into the cavity of the resonance ionization laser ion source [4]. The desired Tl isotopes were ionized with the resonant laser ionization technique. After selective laser photoionization, the radioactive Tl ions were extracted by a 50 kV potential, mass-separated with the General Purpose Separator of ISOLDE and directed into the Windmill (WM) setup [25]. A time gate was used to selectively focus on the decay of short-lived isomer, as will be shown below.

Radioactive ions of ^{183}Tl were implanted in a carbon foil with a 6 mm diameter and 20 μg/cm^2 thickness [29]. The implantation position was surrounded with two partially depleted silicon detectors for detection of α particles and conversion electrons. An annular detector with thickness of 300 μm and area of 450 mm^2 was placed 7 mm upstream from the foil. The beam passed through the hole with 8 mm diameter. Another silicon detector with thickness of 500 μm and area of 300 mm^2 was placed downstream from the foil. Both detectors with typical energy resolution of approximately 25 keV (for both α particles and conversion electrons) covered a solid angle of 24% of 4π. Calibration data for these silicon detectors were taken using the two ^{241}Am sources mounted inside of the WM system.

Two coaxial germanium detectors with relative efficiencies of approximately 70% and 90% were used to detect γ rays. They were placed outside of the vacuum chamber of the WM system at $0°$ and $90°$, relative to the beam direction. Energy and efficiency calibrations were performed using standard radioactive sources of ^{133}Ba, ^{137}Cs, ^{60}Co, and ^{152}Eu. Signals from the preamplifiers of the detectors were processed with a digital data acquisition system, based on commercial Digital Gamma Finder (DGF) modules.

III. EXPERIMENTAL RESULTS

A. Internal transition decay of ^{183m}Tl

The ^{183m}Tl ions were released from the target in only a short period after the proton-pulse impact. Two time gates were used in the following analyses: 0–450 ms ('pulse') and 550–1000 ms ('background') after the proton-pulse impact. Events detected within the 'pulse' gate were dominantly due to a radiation emitted by ^{183m}Tl, while events detected within the 'background' gate were due to long-lived daughter decays and room background.
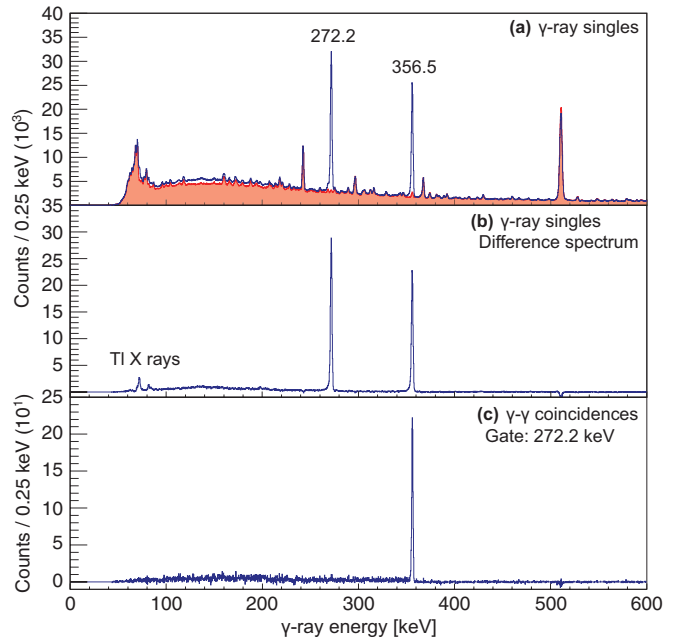

FIG. 2. (a) Singles γ-ray energy spectra detected within the 'pulse' gate and within the 'background' gate (red shaded spectrum). (b) Difference of two previous spectra. (c) Background-subtracted γ-ray energy spectrum, detected in prompt coincidence with the 272.2 keV transition.

Figure 2(a) gives singles γ-ray spectra, detected within the 'pulse' and 'background' (red shaded spectrum) time gates. The difference of both spectra, i.e., spectrum of γ-ray singles attributed to the decay of ^{183m}Tl, is given in Fig. 2(b). Strong γ rays with energies 272.2(2) and 356.5(2) keV, together with characteristic Tl x rays are observed. While, the 272.2 keV γ ray is the known $3/2^+ \rightarrow 1/2^+$ transition in ^{183}Tl [28], this is the first ever evidence for the 356.5 keV transition. The analysis below shows that it is the $9/2^- \rightarrow 3/2^+$ $E3$ transition in ^{183}Tl.

Figure 2(c) gives the spectrum of γ rays detected in prompt $[\Delta t(\gamma_1\text{-}\gamma_2) \leqslant 400$ ns] coincidence with the 272.2 keV transition. Strong coincidence with the 356.5 keV γ ray is observed, thus the 272.2 and 356.5 keV transitions form a cascade. The sum of energies of both γ rays establishes the excitation energy of the isomeric state of 628.7(3) keV. This is in agreement with the previously reported value of 625(7) keV [28].

Figure 3 gives the spectra of conversion electrons (CE) from the 272.2(2) and 356.5(2) keV transitions. Note that they will be discussed below.

Figure 4 gives a time distribution for the 272.2 keV γ ray, measured relative to the proton-pulse impact. Significant deviation from an exponential decay is observed. This is due to high count rates, which caused a slow buffer read-outs of the DGF cards resulting in a dead time effect, see [24,30] for details. Therefore, the distribution was not used to extract the half-life of ^{183m}Tl. However, a fit of a short exponential part (80–125 ms range, indicated with dashed lines in Fig. 4) gives a half-life of 55(3) ms, which is consistent with previously determined half-life of 53.3(3) ms [9] for ^{183m}Tl.
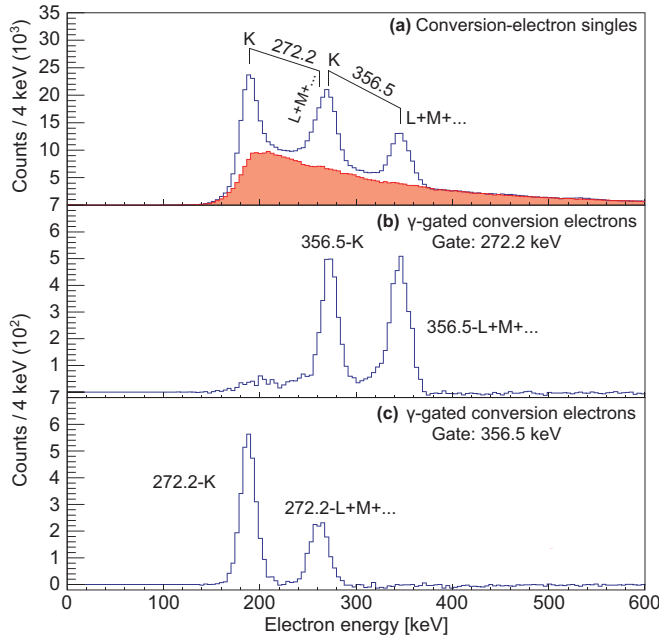
FIG. 3. (a) Singles conversion-electron energy spectra detected within the 'pulse' and 'background' (red shaded spectrum) gates. (b) Background-subtracted conversion-electron energy spectrum detected in prompt coincidence with the 272.2 keV transition. (c) Background-subtracted conversion-electron energy spectrum detected in prompt coincidence with the 356.5 keV transition.

The decay scheme of ^{183m}Tl proposed in the present work is given in Fig. 5. Note that multipolarities of 272.2 and 356.5 keV transitions are determined in further text, together with analysis of the α-decay branch.

Figure 3(a) gives the singles CE spectrum, detected with the 500 μm silicon detector, within the 'pulse' and 'background' (red shaded spectrum) time gates. The three peaks seen in Fig. 3(a) are interpreted as CE from the
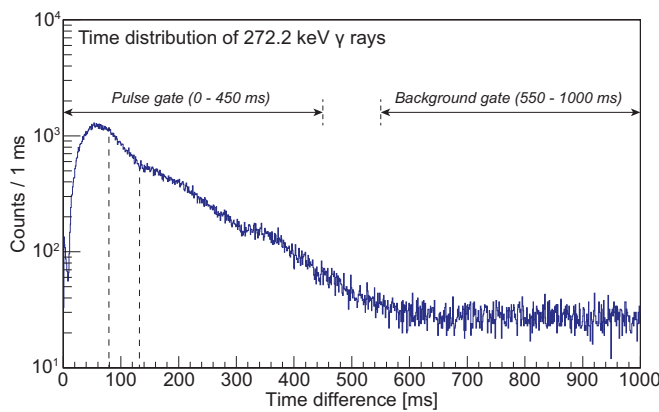

FIG. 4. Time distribution of the 272.2 keV γ-ray events with respect to the proton-pulse impact. A 'pulse' gate was used to identify radiation that arises from the decay of ^{183m}Tl and a 'background' gate for a subtraction of long-lived activities and room background. Vertical dashed lines indicates the range, where the fit with an exponential decay was possible, see text for details.

TABLE I. Experimental and theoretical values of total internal conversion coefficients (α_T) for the 272.2 keV transition, ratios of K-shell (α_K) and $L + M + N + \ldots$-shell ($\alpha_{L+M+N+\ldots}$) internal conversion coefficients for the 272.2 and 356.5 keV transitions. Theoretical values for different multipolarities were calculated with the BrIcc software [31].

| Multipolarity | α_K / $\alpha_{L+M+N+\ldots}$ | | α_T |
	356.5 keV	272.2 keV	272.2 keV
Experiment	0.70(10)	1.94(28)	0.24(2)
$E1$	4.68	4.55	0.04
$M1$	4.56	**4.53**	**0.51**
$E2$	1.72	**1.19**	**0.15**
$M2$	3.32	3.04	2.04
$E3$	**0.61**	0.32	0.90
$M3$	2.07	1.62	7.13
$E4$	0.27	0.12	5.60
$M4$	1.21	0.81	27.73

272.2 and 356.5 keV transitions. Note that K-CE from the 356.5 keV transition and $L + M + \ldots - $CE from the 272.2 keV transition are unresolved. To determine multipolarities of both transitions, γ-gated electron spectra were investigated. Figure 3(b) gives the CE spectrum detected in prompt coincidence with the 272.2 keV γ rays. Assuming the same detection efficiencies for $K - $CE and $L + M + \ldots - $CE, the ratio of internal conversion coefficients $\alpha_K/\alpha_{L+M+N\ldots} = 0.70(10)$ was determined for the 356.5 keV transition. Based on a good agreement with the theoretical value of 0.61, calculated with the BrICC software [31], an $E3$ multipolarity was established unambiguously for the 356.5 keV transition. Theoretical values for other multipolarities are given in Table I.

Figure 3(c) gives the CE spectrum detected in prompt coincidence with the 356.5 keV γ rays. The ratio $\alpha_K/\alpha_{L+M+N\ldots} = 1.94(28)$ was determined for the 272.2 keV transition. This suggests a mixed $M1 + E2$ character for the transition, since the theoretical values are 4.53 for a pure $M1$ and 1.19 for a pure $E2$ multipolarities.

The intensity balance of the 272.2 keV and 356.5 keV γ-rays singles was used to determine the total internal conversion coefficient for the 272.2 keV transition. The internal conversion is interpreted as missing γ-ray intensity. The total conversion coefficient $\alpha_T = 0.24(2)$ was determined for the 272.2 keV transition. This corroborates the above conclusion on the mixed $M1 + E2$ character of the transition, since theoretically $\alpha_T(M1) = 0.51$ and $\alpha_T(E2) = 0.15$. Other multipolarities are excluded, see Table I. Using a combination of both approaches, the $M1/E2$ mixing ratio $\delta = 1.87^{+0.28}_{-0.21}$ was determined with the BrIccMixing software [31].

B. The α decay of ^{183m}Tl

To identify α decays of ^{183m}Tl, the same method, based on the time structure of the data, was employed. Figure 6 gives the spectra of α-decay events detected with silicon detectors within the 'pulse' and 'background' (red shaded spectrum) time gates. The ^{183m}Tl dominantly de-excites through a γ-ray
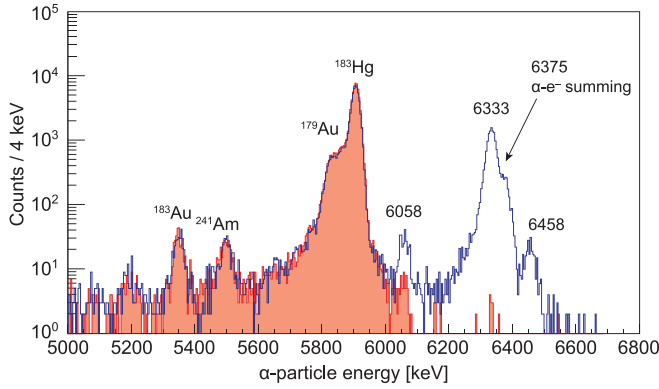
FIG. 5. Decay scheme of ^{183m}Tl deduced in the present work. Note that excitation energy of the 127(17) keV state in ^{179}Au has been determined as the difference in α-particle energies and therefore it has a large experimental uncertainty. The same applies for the 407(17) keV state. For the α decay branching ratio, a weighted average of the value determined here and that taken from [28] is given. The half-life for ^{183m}Tl is taken from [9], since the value determined here is less accurate, see the text for details. The data for $3/2^+$, $3/2^-$, and $5/2^-$ states in ^{179}Au are taken from [19]. Values deduced or improved in the present work are highlighted with red color.

cascade to the ground state, which decays into ^{183}Hg ($T_{1/2} = 9.4(7)$ s [22]). Due to its long half-life, ^{183}Hg appears in both time gates. The same applies also to ^{179}Au ($T_{1/2} = 7.1(3)$ s [27]), which is a product of the α decay of ^{183m}Tl.

Three α decays with energies of 6058(15), 6333(9), and 6458(15) keV are clearly separated from the red spectrum, therefore they are assigned as decays of ^{183m}Tl. The 6333 keV

α decay is the known transition feeding the $9/2^-$ state in ^{179}Au [19]. De-excitation of the $9/2^-$ state proceeds via so-far unobserved low-energy electromagnetic transitions, through an elusive $5/2^-$ state, feeding the $3/2^-$ isomer in ^{179}Au [19]. It was shown that the 6333 keV α decay is strongly affected with an α-electron summing effect, see the discussion in [19]. This leads to an artificial peak observed at approximately

FIG. 6. Singles α-particle energy spectra detected within the 'pulse' and 'background' (red shaded spectrum) gates. α decays of ^{183m}Tl are annotated with energies given in keV. The ^{241}Am peak is from calibration standard that was placed inside of the vacuum chamber of the Windmill system.

6375 keV. This effect is more obvious in both studies at the RITU separator [9,19]. In these experiments, the activity was implanted in the silicon detector, thus the summing probability was much higher.

The weak 6458 keV α decay has $Q_\alpha = 6602(15)$ keV. This agrees with $Q_\alpha = 6604(9)$ keV expected for a direct α decay from ^{183m}Tl to the ^{179}Au ground state. The latter value is based on mass values for ground states of both isotopes taken from [32] and the excitation energy of ^{183m}Tl determined in the present work. Therefore, the 6458 keV α decay is interpreted as a direct feeding of the ground state of ^{179}Au. The difference of Q_α values for the 6333 and 6458 keV α decays establishes an excitation energy of 127(17) keV for the known $9/2^-$ state in ^{179}Au. Within experimental uncertainties, this value agrees with the previously reported value of 134(15) keV [19]. Note that this decay, with slightly different energies has been reported in [9,18], but it was not correctly interpreted.

The 6058 keV transition is reported for the first time here. Figure 7 gives the spectrum of γ rays, detected in prompt $[|\Delta t(\alpha\text{-}\gamma)| \leqslant 1 \ \mu s]$ coincidence with the 6058 keV α decay. Although the statistics are low, a γ ray with an energy of 279.8(5) keV is evident. Weak Au K x rays, together with the 62.4 keV γ ray, which is the known $3/2^- \rightarrow 3/2^+$ transition in ^{179}Au, are also observed. The difference in Q_α values for
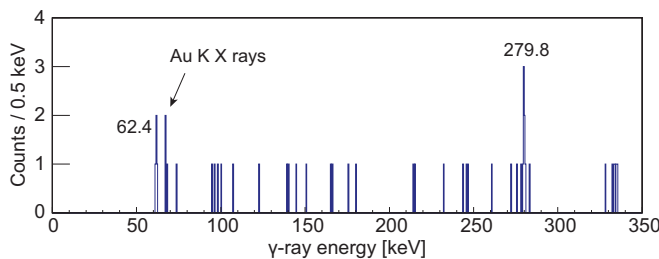

FIG. 7. Spectrum of γ rays, detected in prompt coincidence with the 6058 keV α decay. Only events that occurred within the 'pulse' gate were accepted.

TABLE II. Summary of α decays of ^{183m}Tl characterized in the present work: α-decay energies (E_α), α-decay intensities (I_α), reduced transition widths (δ_α^2), and hindrance factors (HF), given relative to the 6333 keV decay.

E_α [keV]	I_α [%]	δ_α^2 [keV]	HF
6058(15)	1.6(3)	8(2)	5(2)
6333(9)	97.3(11)	39(9)	1
6458(15)	1.1(3)	0.14(4)	279(102)

the 6058 and 6333 keV α decays establishes an excitation energy of a 276(15) keV, relative to the known $9/2^-$ state, for a hitherto unknown state. This corresponds with the observed γ-ray energy of 279.8 keV. Therefore, this γ ray is interpreted as a transition connecting a newly discovered 407(17) keV excited state in ^{179}Au with the known $9/2^-$ state. The new excited state is populated directly by the 6058 keV α decay.

Characteristic Au K X rays observed in the spectrum given in Fig. 7 occur due to K-shell internal conversion of 89.5 and 279.8 keV transitions. The known 89.5 keV $E1$ transition, feeding the ground state, is not observed, since it is 12.2(5) times weaker [19] than the 62.4 keV transition. Using number of observed counts of the 62.4 keV γ rays, the γ-ray intensities given in [19], internal conversion coefficient and x rays fluorescence yields, 0.06(4) counts in the $K_{\alpha 1}$ peak are expected to occur in Fig. 7 due to internal conversion of the 89.5 keV transition. Thus, the influence of the 89.5 keV transition is negligible and observed Au K X rays are almost exclusively due to internal conversion of the new 279.8 keV transition. Therefore, a rough estimation of the K-shell internal conversion coefficient for the 279.8 keV transition could be made using the number of counts of K x rays and γ rays. After correction for respective detection efficiencies and x rays fluorescence yield, $\alpha_K = 1.2^{+1.2}_{-0.8}$ was obtained.

Assuming that the 279.8 keV transition is a dominant de-excitation of the 407 keV state, a total internal conversion coefficient $\alpha_T = 1.0(8)$ for the 279.8 keV transition was obtained by comparing the number of observed 6058 keV α decays in Fig. 6 and the 279.8 keV α-γ coincidences in Fig. 7, corrected for respective detection efficiencies. The large experimental uncertainties of both values do not allow an unambiguous multipolarity assignment for the 279.8 keV transition.

Based on the number of observed α decays in Fig. 6, the intensities of particular transitions were determined: 97.3(11)% for the 6333 keV transition, 1.6(3)% for the 6058 keV transition and 1.1(3)% for the 6458 keV transition. Table II gives a summary of α-decay transitions from ^{183m}Tl that were deduced in the present work. Reduced α-decay widths δ_α^2 and hindrance factors (HF) are determined and discussed in the following section.

Based on the number of observed α decays of ^{183m}Tl in Fig. 6 and of the 356.5 keV γ rays in Fig. 2, corrected for respective detection efficiencies, $b_\alpha = 1.4(3)\%$ and $b_{IT} = 98.6(3)\%$ were deduced for ^{183m}Tl from the present data. This is in a good agreement with the previously reported value $b_\alpha = 1.5(3)\%$ [28]. The weighted average of both values

gives $b_\alpha = 1.45(42)\%$ and thus $b_{IT} = 98.55(42)\%$. These values were used in the decay scheme given in Fig. 5.

IV. DISCUSSION

In the present work, a $M1/E2$ mixing ratio of $\delta = 1.87^{+0.28}_{-0.21}$, was determined for the $3/2^+ \to 1/2^+$ transition in ^{183}Tl. This agrees with the trend established for heavier isotopes, where mixing ratios are in the 1.6–2.3 range, see Fig. 1.

A cascade of γ rays, de-exciting ^{183m}Tl was observed. This involves unambiguous identification of the $E3$ transition with a reduced transition probability $B(E3) = 0.012(1)$ W.u. Although systematic information on reduced transition probabilities of $E3$ transitions in neutron-deficient isotopes is incomplete, see Fig. 1, the $B(E3)$ determined for ^{183}Tl agrees with known values for ^{195,197,201,203}Tl, that are in the 0.0098–0.014 W.u. range. This, together with the above deduced mixing ratio for the $3/2^+ \to 1/2^+$ transition, indicates that very little is changing in the intrinsic structure of the underlying configurations in odd-mass Tl isotopes over a broad range of neutron numbers.

Reduced α-decay widths were calculated using the Rasmussen prescription [33]. For the strongest 6333 keV α decay, a reduced α-decay width of $\delta^2_\alpha = 39(9)$ keV was obtained. This is slightly lower than $\delta^2_\alpha = 59(4)$ keV of an unhindered $0^+ \to 0^+$ α decay of the neighboring even-even ^{182}Hg isotope. This confirms an unhindered character of the 6333 keV α decay, as it has been suggested in [19]. Therefore, a hindrance factor of 1 is assumed for this α decay. The 6333 keV α decay feeds the 127(17) keV $9/2^-$ state in ^{179}Au, which is associated with the $1h_{9/2}$ proton-intruder configuration [34,35], coupled with the 0^+ ground state of the ^{178}Pt core.

Another $9/2^-$ state is expected to occur in ^{179}Au, due to coupling of the $1h_{9/2}$ proton with the 0^+ excited state ($E^* = 421.0(6)$ keV [36]) in the ^{178}Pt core. Note that such pairs of $9/2^-$ states, together with linking $E0$ transitions, were reported for ^{185,187}Au [37]. A reduced α-decay width of $\delta^2_\alpha = 8(2)$ keV was determined for the 6058 keV α decay, which feeds the 407(17) keV state. A hindrance factor HF = 5(2) was calculated relative to the unhindered 6333 keV α decay. The slight hindrance suggests a $\Delta L = 0$ character for the 6058 keV α decay and thus a tentative $(9/2^-)$ spin-parity assignment is made for the 407(17) keV state.

Proton-intruder states in ^{183}Tl and ^{179}Au occur due to coupling of the odd-proton with states in the ^{182}Hg and ^{178}Pt cores. Therefore, ^{183m}Tl $\to$ ^{179}Au and ^{182}Hg^m $\to$ ^{178}Pt were compared. Figure 8 gives a partial α-decay schemes for ^{183m}Tl and ^{182}Hg, together with the hindrance factors for respective transitions. The 5446 keV α decay of ^{182}Hg feeds the excited 0^+ state in ^{178}Pt. A hindrance factor of 3.5(6) has been determined for this α decay [36]. The slight hindrance is explained by a weak mixing of 0^+ states in ^{182}Hg and a strong mixing of 0^+ states in ^{178}Pt [38]. The decay pattern observed for ^{183m}Tl appears to be similar, since a prolate-oblate mixing has been proposed for the initial state [1,7]. Therefore, the 407(17) keV excited state is a good candidate for the expected coexisting $9/2^-$ structure, i.e., coupling of $1h_{9/2}$ proton with the excited 0^+ state in ^{178}Pt. A more precise dataset needs to
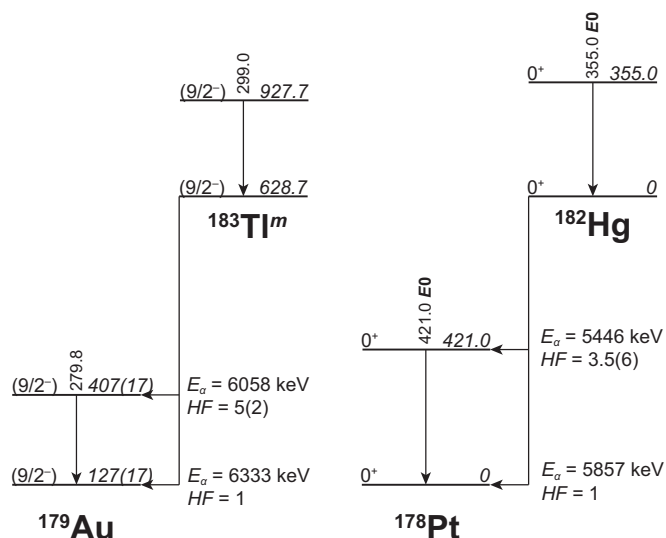

FIG. 8. Partial α-decay schemes for ^{183m}Tl and ^{182}Hg. Hindrance factors (HF) for α-decay transitions are given. The data for ^{182}Hg are taken from [36].

be acquired before an unambiguous conclusion can be made. Most important would be to identify an $E0$ component of the 279.8 keV transition.

A spin-parity of the ground state of ^{179}Au has been unambiguously assigned as $1/2^+$ [39]. A reduced α-decay width of $\delta^2_\alpha = 0.14(4)$ keV was determined for the 6458 keV α decay. Relative to the unhindered 6333 keV transition, this gives HF = 279(102). Similar $9/2^- \to 1/2^+$ decays were identified in ^{189,191,193,195}Bi [40]. Their hindrance factors are in the range of 300–700. The value established for the ^{183m}Tl α decay is consistent with this range and thus it corroborates the $9/2^- \to 1/2^+$ interpretation for the 6458 keV α decay.

V. CONCLUSION

The internal transition decay and α decay of mass-separated samples of ^{183m}Tl have been studied at the ISOLDE facility at CERN. The new results include the first identification of an $E3$ transition feeding the $3/2^+$ state in ^{183}Tl and measurement of a $M1/E2$ mixing ratio for the $3/2^+ \to 1/2^+$ transition. Measurements of the $M1/E2$ mixing ratios are of particular interest, since they allow extraction of the reduced transition probabilities for both electromagnetic components, if the half-life of the initial state is known. This is not the case of the $3/2^+$ state in ^{183}Tl, however, its half-life can be measured using, e.g., fast-timing LaBr$_3$(Ce) detectors. Then, using the $M1/E2$ mixing ratio determined in the present work, absolute values of $B(M1)$ and $B(E2)$ could be extracted. These mixing ratios are very sensitive to nuclear deformation, both axial and triaxial.

Three α decays of ^{183m}Tl have been characterized. This involves a new decay path, which populates a previously unknown excited state in ^{179}Au. It decays via a transition that might have a significant $E0$ component, which is a model independent signature of shape coexistence [41]. Therefore it is a candidate for the coexisting $9/2^-$ state, similar to those

observed in ^{185,187}Au. Systematic evolution of excitation energies and decay properties of these structures beyond $N = 104$ midshell point is unknown. Weak α decays of odd-mass Tl isotopes appear to be a suitable tool to study these structures in neutron-deficient odd-Au isotopes.

ACKNOWLEDGMENTS

[1] K. Heyde and J. L. Wood, Rev. Mod. Phys. **83**, 1467 (2011).

[2] K. Heyde, P. Van Isacker, M. Waroquier, J. Wood, and R. Meyer, Phys. Rep. **102**, 291 (1983).

[3] J. Wood, K. Heyde, W. Nazarewicz, M. Huyse, and P. van Duppen, Phys. Rep. **215**, 101 (1992).

[4] V. Fedosseev, K. Chrysalidis, T. D. Goodacre, B. Marsh, S. Rothe, C. Seiffert, and K. Wendt, J. Phys. G: Nucl. Part. Phys. **44**, 084006 (2017).

[5] A. N. Andreyev, S. Antalic, D. Ackermann, T. E. Cocolios, V. F. Comas, J. Elseviers, S. Franchoo, S. Heinz, J. A. Heredia, F. P. Heßberger, S. Hofmann, M. Huyse, J. Khuyagbaatar, I. Kojouharov, B. Kindler, B. Lommel, R. Mann, R. D. Page, S. Rinta-Antila, P. J. Sapple *et al.*, Phys. Rev. C **80**, 024302 (2009).

[6] A. E. Barzakh, L. K. Batist, D. V. Fedorov, V. S. Ivanov, K. A. Mezilev, P. L. Molkanov, F. V. Moroz, S. Y. Orlov, V. N. Panteleev, and Y. M. Volkov, Phys. Rev. C **88**, 024315 (2013).

[7] A. E. Barzakh, A. N. Andreyev, T. E. Cocolios, R. P. de Groote, D. V. Fedorov, V. N. Fedosseev, R. Ferrer, D. A. Fink, L. Ghys, M. Huyse, U. Köster, J. Lane, V. Liberati, K. M. Lynch, B. A. Marsh, P. L. Molkanov, T. J. Procter, E. Rapisarda, S. Rothe, K. Sandhu *et al.*, Phys. Rev. C **95**, 014324 (2017).

[8] G. Lane, G. Dracoulis, A. Byrne, P. Walker, A. Baxter, J. Sheikh, and W. Nazarewicz, Nucl. Phys. A **586**, 316 (1995).

[9] P. M. Raddon, D. G. Jenkins, C. D. O'Leary, A. J. Simons, R. Wadsworth, A. N. Andreyev, R. D. Page, M. P. Carpenter, F. G. Kondev, T. Enqvist, P. T. Greenlees, P. M. Jones, R. Julin, S. Juutinen, H. Kettunen, M. Leino, A.-P. Leppänen, P. Nieminen, J. Pakarinen, P. Rahkila *et al.*, Phys. Rev. C **70**, 064308 (2004).

[10] M.-G. Porquet, A. J. Kreiner, F. Hannachi, V. Vanin, G. Bastin, C. Bourgeois, J. Davidson, M. Debray, G. Falcone, A. Korichi, H. Mosca, N. Perrin, H. Sergolle, F. A. Beck, and J.-C. Merdinger, Phys. Rev. C **44**, 2445 (1991).

[11] W. Reviol, L. L. Riedinger, J. M. Lewis, W. F. Mueller, C. R. Bingham, J. Y. Zhang, and B. E. Zimmerman, Phys. Scr. **T56**, 167 (1995).

[12] F. G. Kondev, Nucl. Data Sheets **108**, 365 (2007).

[13] B. Singh, Nucl. Data Sheets **108**, 79 (2007).

[14] X. Huang and C. Zhou, Nucl. Data Sheets **104**, 283 (2005).

[15] X. Huang and M. Kang, Nucl. Data Sheets **121**, 395 (2014).

[16] M. Shamsuzzoha Basunia, Nucl. Data Sheets **143**, 1 (2017).

[17] E. Achterberg, O. Capurro, G. Marti, V. Vanin, and R. Castro, Nucl. Data Sheets **107**, 1 (2006).

[18] U. Schrewe, P. Tidemand-Petersson, G. Gowdy, R. Kirchner, O. Klepper, A. Płochocki, W. Reisdorf, E. Roeckl, J. Wood, J. Żylicz, R. Fass, and D. Schardt, Phys. Lett. B **91**, 46 (1980).

[19] M. Venhart, A. N. Andreyev, J. L. Wood, S. Antalic, L. Bianco, P. T. Greenlees, U. Jakobsson, P. Jones, R. Julin, S. Juutinen, S. Ketelhut, M. Leino, M. Nyman, R. D. Page, P. Peura, P. Rahkila, J. Sarén, C. Scholey, J. Sorri, J. Thomson *et al.*, Phys. Lett. B **695**, 82 (2011).

[20] K. Toth, M. Ijaz, J. Lin, E. Robinson, B. Hannah, E. Spejewski, J. Cole, J. Hamilton, and A. Ramayya, Phys. Lett. B **63**, 150 (1976).

[21] E. Rapisarda, A. N. Andreyev, S. Antalic, A. Barzakh, T. E. Cocolios, I. G. Darby, R. D. Groote, H. D. Witte, J. Diriken, J. Elseviers, D. Fedorov, V. N. Fedosseev, R. Ferrer, M. Huyse, Z. Kalaninová, U. Köster, J. Lane, V. Liberati, K. M. Lynch, B. A. Marsh *et al.*, J. Phys. G: Nucl. Part. Phys. **44**, 074001 (2017).

[22] C. M. Baglin, Nucl. Data Sheets **134**, 149 (2016).

[23] B. Andel, A. N. Andreyev, S. Antalic, A. Barzakh, N. Bree, T. E. Cocolios, V. F. Comas, J. Diriken, J. Elseviers, D. V. Fedorov, V. N. Fedosseev, S. Franchoo, L. Ghys, J. A. Heredia, M. Huyse, O. Ivanov, U. Köster, V. Liberati, B. A. Marsh, K. Nishio *et al.*, and Phys. Rev. C **96**, 054327 (2017).

[24] C. Van Beveren, A. N. Andreyev, A. E. Barzakh, T. E. Cocolios, D. Fedorov, V. N. Fedosseev, R. Ferrer, M. Huyse, U. Köster, J. Lane, V. Liberati, K. M. Lynch, B. A. Marsh, T. J. Procter, D. Radulov, E. Rapisarda, K. Sandhu, M. D. Seliverstov, P. Van Duppen, M. Venhart *et al.*, Phys. Rev. C **92**, 014325 (2015).

[25] C. V. Beveren, A. N. Andreyev, A. E. Barzakh, T. E. Cocolios, R. P. de Groote, D. Fedorov, V. N. Fedosseev, R. Ferrer, L. Ghys, M. Huyse, U. Köster, J. Lane, V. Liberati, K. M. Lynch, B. A. Marsh, P. L. Molkanov, T. J. Procter, E. Rapisarda, K. Sandhu, M. D. Seliverstov *et al.*, J. Phys. G: Nucl. Part. Phys. **43**, 025102 (2016).

[26] J. Elseviers, A. N. Andreyev, S. Antalic, A. Barzakh, N. Bree, T. E. Cocolios, V. F. Comas, J. Diriken, D. Fedorov, V. N. Fedosseyev, S. Franchoo, J. A. Heredia, M. Huyse, O. Ivanov, U. Köster, B. A. Marsh, R. D. Page, N. Patronis, M. Seliverstov, I. Tsekhanovich *et al.*, Phys. Rev. C **84**, 034307 (2011).

[27] C. M. Baglin, Nucl. Data Sheets **110**, 265 (2009).

[28] A. N. Andreyev, S. Antalic, D. Ackermann, S. Franchoo, F. P. Heßberger, S. Hofmann, M. Huyse, I. Kojouharov, B. Kindler, P. Kuusiniemi, S. R. Lesher, B. Lommel, R. Mann, G. Münzenberg, K. Nishio, R. D. Page, J. J. Ressler, B. Streicher, S. Saro, B. Sulignano *et al.*, Phys. Rev. C **73**, 044324 (2006).

[29] B. Lommel, W. Hartmann, B. Kindler, J. Klemm, and J. Steiner, Nucl. Instrum. Methods Phys. Res. A **480**, 199 (2002).

[30] C. Van Beveren, Laser-assisted decay and optical spectroscopy studies of neutron-deficient thallium isotopes, doctoral thesis, KU Leuven, Belgium, 2016.

[31] T. Kibédi, T. Burrows, M. Trzhaskovskaya, P. Davidson, and C. Nestor, Nucl. Instrum. Methods Phys. Res. A **589**, 202 (2008).

[32] M. Wang, G. Audi, F. G. Kondev, W. Huang, S. Naimi, and X. Xu, Chin. Phys. C **41**, 030003 (2017).

[33] J. O. Rasmussen, Phys. Rev. **113**, 1593 (1959).

[34] W. F. Mueller, W. Reviol, M. P. Carpenter, R. V. F. Janssens, F. G. Kondev, K. Abu Saleem, I. Ahmad, H. Amro, C. R. Bingham, J. Caggiano, C. N. Davids, D. Hartley, A. Heinz, B. Herskind, D. Jenkins, T. L. Khoo, T. Lauritsen, W. C. Ma, J. Ressler, L. L. Riedinger *et al.*, Phys. Rev. C **69**, 064315 (2004).

[35] M. Venhart, M. Balogh, A. Herzáň, J. Wood, F. Ali, D. Joss, A. Andreyev, K. Auranen, R. Carroll, M. Drummond, J. Easton, P. Greenlees, T. Grahn, A. Gredley, J. Henderson, U. Jakobsson, R. Julin, S. Juutinen, J. Konki, E. Lawrie *et al.*, Phys. Lett. B **806**, 135488 (2020).

[36] J. Wauters, P. Dendooven, M. Huyse, G. Reusen, P. Van Duppen, R. Kirchner, O. Klepper, and E. Roeckl, Z. Phys. A: At. Nucl. **345**, 21 (1993).

[37] C. D. Papanicolopulos, M. A. Grimm, J. L. Wood, E. F. Zganjar, M. O. Kortelahti, J. D. Cole, and H. K. Carter, Z. Phys. A: At. Nucl. **330**, 371 (1988).

[38] J. Wauters, N. Bijnens, H. Folger, M. Huyse, H. Y. Hwang, R. Kirchner, J. von Schwarzenberg, and P. Van Duppen, Phys. Rev. C **50**, 2768 (1994).

[39] J. G. Cubiss, A. E. Barzakh, A. N. Andreyev, M. Al Monthery, N. Althubiti, B. Andel, S. Antalic, D. Atanasov, K. Blaum, T. E. Cocolios, T. Day Goodacre, R. P. de Groote, A. de Roubin, G. J. Farooq-Smith, D. V. Fedorov, V. N. Fedosseev, R. Ferrer, D. A. Fink, L. P. Gaffney, L. Ghys *et al.*, Phys. Lett. B **786**, 355 (2018).

[40] E. Coenen, K. Deneffe, M. Huyse, P. Van Duppen, and J. L. Wood, Phys. Rev. Lett. **54**, 1783 (1985).

[41] J. Wood, E. Zganjar, C. De Coster, and K. Heyde, Nucl. Phys. A **651**, 323 (1999).